nature photonics

LETTERS

https://doi.org/10.1038/s41566-019-0527-y

Broadband reduction of quantum radiation pressure noise via squeezed light injection

Min Jet Yap[1*], Jonathan Cripe[2], Georgia L. Mansell[1,6], Terry G. McRae[1], Robert L. Ward[1], Bram J. J. Slagmolen[1], Paula Heu[3,4], David Follman[3,4], Garrett D. Cole[3,4,5], Thomas Corbitt[2] and David E. McClelland[1]

The Heisenberg uncertainty principle states that the position of an object cannot be known with infinite precision, as the momentum of the object would then be totally uncertain. This momentum uncertainty then leads to position uncertainty in future measurements. When continuously measuring the position of an object, this quantum effect, known as back-action, limits the achievable precision[1,2]. In audio-band, interferometer-type gravitational-wave detectors, this back-action effect manifests as quantum radiation pressure noise (QRPN) and will ultimately (but does not yet) limit sensitivity[3]. Here, we present the use of a quantum engineered state of light to directly manipulate this quantum back-action in a system where it dominates the sensitivity in the 10–50 kHz range. We observe a reduction of 1.2 dB in the quantum back-action noise. This experiment is a crucial step in realizing QRPN reduction for future interferometric gravitational-wave detectors and improving their sensitivity.

When gravitational wave (GW) detectors such as the Advanced Laser Interferometer Gravitational-Wave Observatory (LIGO)[4], Advanced Virgo[5] and KAGRA[6] reach their design sensitivity, quantum noise will be the dominant noise source across most of the detection band[3]. Quantum noise arises from the quantum nature of the light used to probe the positions of the test masses[2]. The individual photons that comprise a coherent state are uncorrelated, and fluctuations in their rate of arrival obey Poisson statistics. At the point of photodetection, these fluctuations are referred to as shot noise (SN) and they limit the readout sensitivity. At the point when the photons reflect off the test mass, these fluctuations generate a fluctuating momentum transfer to the test mass and perturb its position; this is known as quantum radiation pressure noise, QRPN (or, sometimes, radiation pressure SN).

The injection of squeezed vacuum into the interferometer dark port allows the quantum noise to be manipulated[2]. Phase quadrature squeezed light can reduce SN and has been demonstrated on previous generations of GW detectors at both GEO-600[7,8] and LIGO Hanford[9], and is now in routine operation in current GW detectors. The use of squeezing in the form of amplitude quadrature squeezed light to reduce the fluctuating radiation pressure force and hence QRPN has been demonstrated in a cryogenic microwave optomechanical system near the MHz-regime mechanical resonance frequency[10]. Here, we present a broadband audio-frequency demonstration, at optical wavelength and at room temperature.

As GW detectors approach their design sensitivity, it is important to study the effects of QRPN in relevant optomechanical systems. In addition to the injection of squeezed light, other QRPN mitigation techniques such as variational readout[11], conditional squeezing[12] and the use of negative mass systems[13] have also been proposed to improve the low-frequency sensitivity of GW detectors. The effects of QRPN were first observed with tabletop experiments[10,14–17]. These observations were all made at high frequencies (approximately MHz to GHz), around the resonance of the mechanical oscillator. This is due to the difficulty in reducing thermal and other classical noise sources below the QRPN level at low frequencies.

In contrast, GW detectors will be QRPN-dominated at audio (~10 Hz to kHz) frequencies over a large frequency band away from the ~1 Hz mechanical resonance. A direct measurement of QRPN under such conditions at room temperature has only recently been performed[18,19], enabling the experiment reported here. We investigate the injection of squeezed light in a QRPN-limited optomechanical system, and report the reduction of broadband QRPN at room temperature, away from the optical spring-shifted mechanical resonance and at frequencies relevant to GW detectors.

The optomechanical system shown in Fig. 1 is a Fabry–Pérot cavity with a micro-mechanical oscillator as one of the end mirrors. We use a low-loss single-crystal microresonator with low thermal noise to allow the effects of QRPN to be observed at room temperature. The system is installed on a breadboard suspended by three 150 mm wires inside a vacuum chamber at 10^{-5} Pa in order to provide passive seismic and acoustic isolation. The microresonator consists of a mirror pad (~70 μm diameter) suspended from a single-crystal GaAs cantilever (thickness of 220 nm, width of 8 μm and length of 55 μm). The mirror pad is composed of 23 pairs of quarter-wave optical thickness GaAs/$Al_{0.92}Ga_{0.08}As$ layers for a transmission of $T = 250$ ppm and exhibits both low optical losses and a high mechanical quality factor[20–22]. The microresonator has an effective mass of 50 ng, a natural mechanical frequency of $\Omega_m = 2\pi \times 876$ Hz, and a measured mechanical quality factor of $Q_m = 16{,}000$ at room temperature[18]. The cavity has a length of 9 ± 1 mm, a finesse of $\mathcal{F} \approx 13{,}000$ and linewidth (half-width at half-maximum, HWHM) of $2\pi \times 580$ kHz.

A 1,064 nm Nd:YAG laser is used to probe the optomechanical cavity and is detuned above the cavity resonance frequency, which results in a strong optical spring effect[23]. The optical spring self-locks the cavity for frequencies below the optical spring resonance, but the phase lag due to the finite cavity response results in an

[1]OzGrav, Department of Quantum Science, Research School of Physics, Australian National University, Canberra, Australian Capital Territory, Australia. [2]Department of Physics & Astronomy, Louisiana State University, Baton Rouge, LA, USA. [3]Crystalline Mirror Solutions LLC, Santa Barbara, CA, USA. [4]Crystalline Mirror Solutions GmbH, Vienna, Austria. [5]Vienna Center for Quantum Science and Technology (VCQ), Faculty of Physics, University of Vienna, Vienna, Austria. [6]Present address: LIGO Hanford Observatory/MIT, Richland, WA, USA. *e-mail: minjet.yap@anu.edu.au

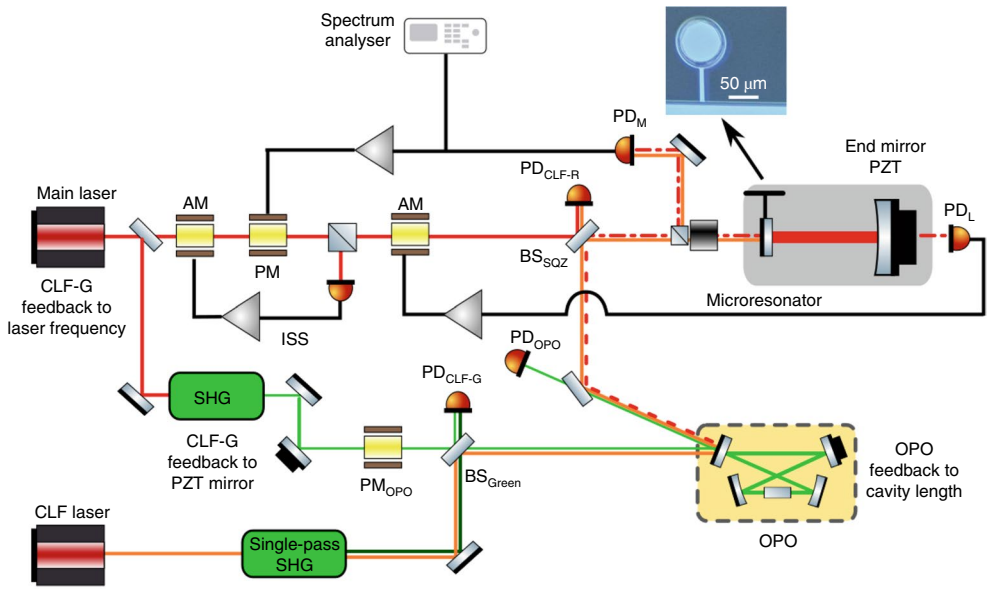

Fig. 1 | Schematic of the experiment. Squeezed vacuum (dashed red line) is generated from an optical parametric oscillator (OPO) pumped by an optical field (light green) at twice the main laser frequency from a second-harmonic generator (SHG). The squeezed vacuum state is then combined with the main laser (red) using a 97:3 beamsplitter (BS_{SQZ}) to produce a bright squeezed state (dotted-dashed red line). The bright squeezed state is injected into the in-vacuum optomechanical cavity, which consists of the microresonator (see inset) and a macroscopic end mirror. The reflected (transmitted) cavity field detected by photodetector PD_M (PD_L) is used to actively stabilize the optomechanical cavity. A secondary coherent locking field (CLF) laser (orange and dark green) is used to control the squeezing quadrature via feedback to the main laser frequency and the OPO pump phase. PZT, piezoelectric transducer.

anti-damping force, rendering the system unstable[24,25]. The optical spring effect is stabilized by monitoring the cavity reflection and transmission field, and providing active feedback around the optical spring frequency to the laser power and frequency via an electro-optic amplitude modulator (AM) and phase modulator (PM)[18,26]. In the final measurement configuration, only the reflected light and PM feedback loop is used to lock the cavity at a detuning of ~0.6 linewidths, with the optical spring increasing the mechanical resonance frequency to 140 kHz.

The squeezed vacuum state is generated from a sub-threshold degenerate OPO via the parametric down-conversion process. The OPO is a doubly resonant bowtie cavity with a nonlinear crystal made of periodically poled potassium titanyl phosphate placed within the cavity, and is pumped by light tapped from the main laser that has been frequency-doubled to 532 nm via an SHG cavity[27,28]. The OPO is kept on resonance with the pump light via radio frequency (RF) reflection locking with 70 MHz sidebands generated from PM_{OPO}, monitored at photodetector PD_{OPO} (Fig. 1). Squeezed light is injected into the cavity by combining the main laser field with the squeezed vacuum state via an asymmetric 97:3 beamsplitter (BS_{SQZ}). Spatial mode mismatch is filtered out by passing the combined field through a short optical fibre before the optomechanical cavity (not shown in the experimental schematic). An intensity stabilization servo (ISS) is used to suppress the main laser down to an out-of-loop relative intensity noise of $2.6\times10^{-8}\,\mathrm{Hz}^{-1/2}$. This results in a greater than 10 dB clearance below the SN level at the optical power of 25 μW used for the final measurement.

Control of the squeezing angle with respect to the main laser is achieved with a coherent locking scheme[29,30] that utilizes a CLF laser frequency-shifted from the main laser by 12.5 MHz. The frequency difference between the two lasers is maintained by upconverting a small portion of the CLF laser to 532 nm and phase-locking the 25 MHz beat note between the upconverted field and the OPO pump field detected at photodetector PD_{CLF-G}. The unconverted (1,064 nm) CLF beam co-propagates with the squeezed vacuum field and is phase-locked with the main laser after BS_{SQZ} at 12.5 MHz,

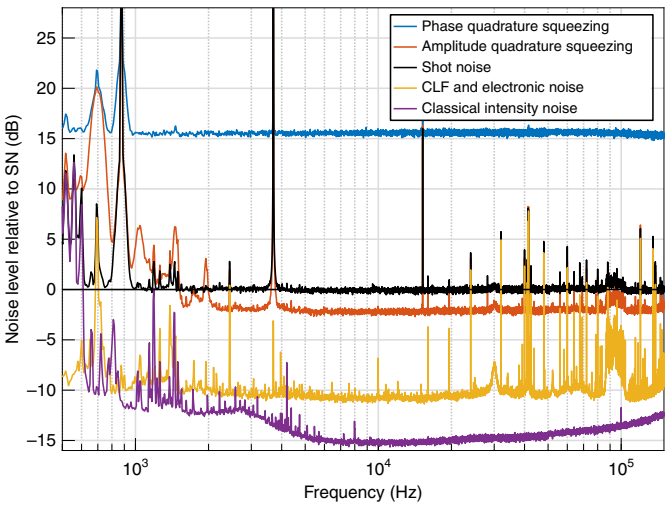

Fig. 2 | Low-frequency squeezed light. Squeezed light noise spectrum measured at the reflection port of the optomechanical cavity, with the cavity highly detuned. The out-of-loop classical laser intensity noise measured at PD_{CLF-R} is projected onto the same plot, and shows >10 dB clearance from the SN. The low-frequency roll up of the amplitude quadrature squeezed spectrum is due to feedback noise coupling from the CLF locking loop.

measured at photodetector PD_{CLF-R}. Engaging both the CLF phase locks allows the squeezing ellipse angle to track the phase of the main laser field. Rotation of the squeezed ellipse between the amplitude and phase quadrature is achieved by changing the demodulation phase between the two CLF phase locks. Figure 2 shows the performance of the squeezer, demonstrating the low frequency at which bright squeezed light has been produced in a nonlinear crystal-based system (see Supplementary Information).

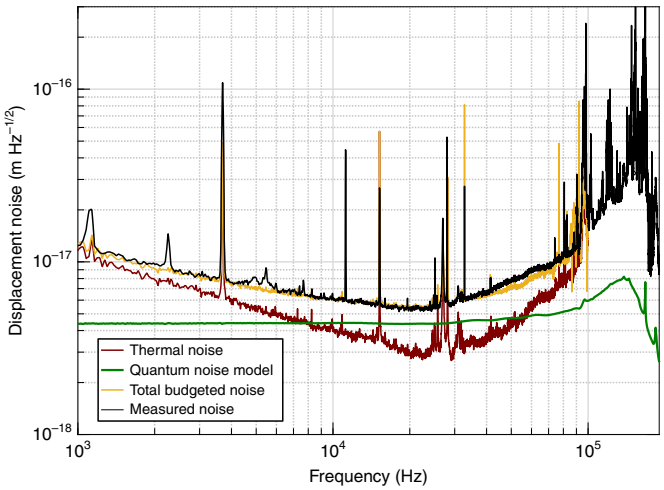

Fig. 3 | Noise budget. Displacement spectral density of the microresonator with a 140 kHz optical spring resonance and the contribution from various noise sources. The dominant noise sources are thermal noise (brown trace) and quantum noise (green trace). The quantum noise is dominated by QRPN below the optical spring resonance. The thermal noise measurement was taken with low intracavity power and closely follows a structural damping model[18]. The quantum noise trace also takes into account the electronic dark noise level of the photodetector. The quadrature sum of the two noise sources (yellow trace) is overlaid with the measured displacement spectrum (black trace) with no squeezed light injection.

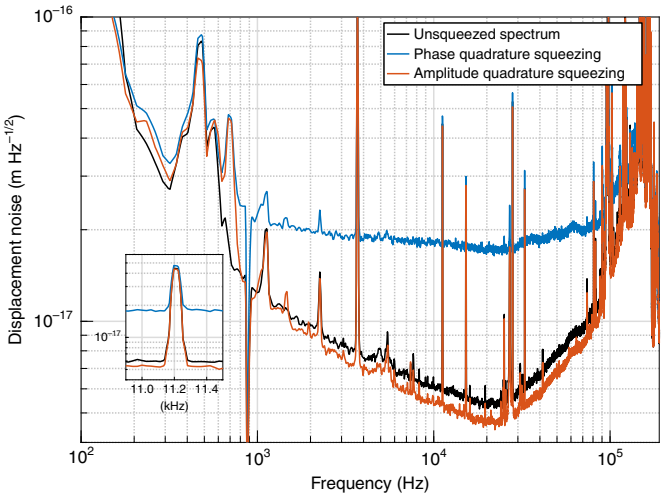

Fig. 4 | Manipulation of QRPN with squeezed light. Calibrated displacement noise spectrum of the microresonator with the injection of squeezed light. The reference trace (black) is measured by tuning the OPO to its anti-resonance to ensure no squeezed light is generated. The injection of amplitude quadrature squeezed light (red) results in a maximum noise reduction of 1.2 dB at 20 kHz. Rotating the squeezed ellipse to the phase quadrature (blue) increased the total noise of the system. Inset: 11.2 kHz calibration line used in the three measurements.

Figure 3 shows the displacement spectral density measured at PD_M with 220 mW of circulating power. The broad peak at 140 kHz is the mechanical fundamental frequency shifted up by the optical spring effect[26]. The dominant noise source below 10 kHz is the thermal noise of the microresonator, which follows a structural damping model between 200 Hz and 30 kHz, and falls off as $1/f^{1/2}$ compared to QRPN[18]. This $1/f^{1/2}$ difference in scaling between the QRPN and thermal noise is what allows the QRPN to dominate above 10 kHz. With 220 mW of circulating power, QRPN is the dominant noise source between 10 kHz and 50 kHz. The excess thermal noise above 30 kHz is believed to be related to thermoelastic damping[18].

The spectrum is calibrated by dividing the measured noise spectrum by the transfer function from the main laser piezo to the cavity reflection port. The laser piezo actuates on the main laser frequency and has been calibrated separately. The transfer function measures the closed-loop response of the system, and undoes the effect of both the electronic feedback and the optical spring response. The optical spring effect is reintroduced in the spectrum by measuring separately the optical spring frequency and cavity detuning. A 11.2 kHz dither tone on the cavity length is used to produce a calibration line, shown in the inset of Fig. 4, to ensure that the calibration is constant for all the measurements. The laser piezo is calibrated in frequency, which allows the spectrum to be calibrated in terms of displacement based on the cavity length.

To manipulate the QRPN, bright squeezed light is injected into the cavity, which affects the measured displacement spectrum as shown in Fig. 4. With the injection of amplitude quadrature squeezed light, we observe a reduction of the total noise floor at frequencies where QRPN is dominant, with a maximum reduction of 1.2 dB at around 20 kHz. Even though thermal noise is the dominant noise source below 10 kHz, QRPN is still a major contributor to the total noise and the reduction in noise due to squeezed light injection remains visible below 2 kHz. By changing the relative phase between the two CLF locks, we are able to rotate the squeezing ellipse to produce phase quadrature squeezed light, resulting in an increase of the total noise by 12.6 dB at 20 kHz. The flat and broadband nature of the increase is consistent with quantum noise being manipulated. Figure 5 shows the noise reduction and enhancement across the measurement spectrum and averaged between 19 and 23 kHz where the largest reduction occurred. The amount of noise reduction observed is currently limited by losses in the system. We estimate, with a pure squeezed state injected into the cavity, the maximum noise reduction is 2.6 dB given the losses in the system. The details of the loss analysis are presented in the Supplementary Information.

We have presented the reduction of QRPN of a microresonator away from the optical spring-shifted mechanical resonance over a broad frequency range via the injection of squeezed light. This is a step towards reducing the radiation pressure noise occurring in future interferometric GW observatories in order to improve their sensitivity and detection range. Moreover, a radiation pressure noise-limited optomechanical system provides a useful testbed for other QRPN reduction proposals[11,19,31–33] and quantum-enhanced displacement sensing[34].

With the optomechanical system at room temperature, the standard quantum limit[35] is currently within a factor of five of the current noise level, with the system predominately dominated by quantum and thermal noise. By cryogenically cooling the microresonator and implementing QRPN cancellation techniques[19] such as utilizing the optical spring[36], this paves the way to reaching and surpassing the standard quantum limit.

Data availability

The data that support the plots within this paper and other findings of this study are available from the corresponding author upon reasonable request.

Online content

Any methods, additional references, Nature Research reporting summaries, source data, statements of code and data availability and associated accession codes are available at https://doi.org/10.1038/s41566-019-0527-y.

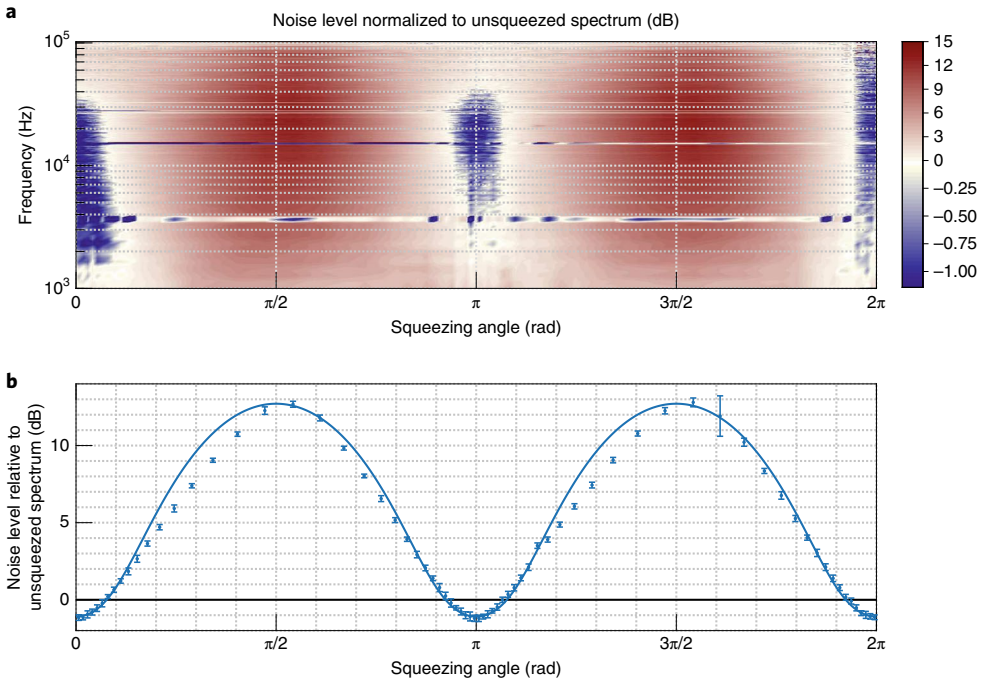

Fig. 5 | Noise level as a function of squeezing angle. a,**b**, Displacement noise spectrum as a function of the squeezing phase, normalized to the reference spectrum across the measurement frequency band (**a**) and averaged between 19 and 23 kHz (**b**). Horizontal lines at 3.7 kHz, 15 kHz and 28 kHz in **a** correspond to the higher-order mechanical modes of the microresonator. Phase quadrature squeezing occurs at π/2 radians, while amplitude quadrature squeezing occurs at π radians. Error bars represent s.d. of the noise level.

Received: 16 April 2019; Accepted: 27 August 2019;
Published online: 07 October 2019

References

1. Braginksky, V. & Vyatchanin, S. Gravitational waves and the limiting stability of self-excited oscillators. *Sov. Phys. JETP* **47**, 433–435 (1978).
2. Caves, C. M. Quantum-mechanical noise in an interferometer. *Phys. Rev. D* **23**, 1693–1708 (1981).
3. Hild, S. Beyond the second generation of laser-interferometric gravitational wave observatories. *Class. Quantum Grav.* **29**, 124006 (2012).
4. The LIGO Scientific Collaboration Advanced LIGO. *Class. Quantum Grav.* **32**, 074001 (2015).
5. The VIRGO Collaboration Advanced Virgo: a second-generation interferometric gravitational wave detector. *Class. Quantum Grav.* **32**, 024001 (2015).
6. The KAGRA Collaboration Detector configuration of KAGRA—the Japanese cryogenic gravitational-wave detector. *Class. Quantum Grav.* **29**, 124007 (2012).
7. The LIGO Scientific Collaboration A gravitational wave observatory operating beyond the quantum shot-noise limit. *Nat. Phys.* **7**, 962–965 (2011).
8. Grote, H. et al. First long-term application of squeezed states of light in a gravitational-wave observatory. *Phys. Rev. Lett.* **110**, 181101 (2013).
9. The LIGO Scientific Collaboration Enhanced sensitivity of the LIGO gravitational wave detector by using squeezed states of light. *Nat. Photon.* **7**, 613–619 (2013).
10. Clark, J. B., Lecocq, F., Simmonds, R. W., Aumentado, J. & Teufel, J. D. Observation of strong radiation pressure forces from squeezed light on a mechanical oscillator. *Nat. Phys.* **12**, 683–687 (2016).
11. Kimble, H. J., Levin, Y., Matsko, A. B., Thorne, K. S. & Vyatchanin, S. P. Conversion of conventional gravitational-wave interferometers into quantum nondemolition interferometers by modifying their input and/or output optics. *Phys. Rev. D* **65**, 022002 (2001).
12. Ma, Y. et al. Proposal for gravitational-wave detection beyond the standard quantum limit through EPR entanglement. *Nat. Phys.* **13**, 776–780 (2017).
13. Khalili, F. Y. & Polzik, E. S. Overcoming the standard quantum limit in gravitational wave detectors using spin systems with a negative effective mass. *Phys. Rev. Lett.* **121**, 031101 (2018).
14. Purdy, T. P., Peterson, R. W. & Regal, C. A. Observation of radiation pressure shot noise on a macroscopic object. *Science* **339**, 801–804 (2013).
15. Teufel, J. D., Lecocq, F. & Simmonds, R. W. Overwhelming thermomechanical motion with microwave radiation pressure shot noise. *Phys. Rev. Lett.* **116**, 013602 (2016).
16. Purdy, T. P., Grutter, K. E., Srinivasan, K. & Taylor, J. M. Quantum correlations from a room-temperature optomechanical cavity. *Science* **356**, 1265–1268 (2017).
17. Sudhir, V. et al. Quantum correlations of light from a room-temperature mechanical oscillator. *Phys. Rev. X* **7**, 031055 (2017).
18. Cripe, J. et al. Measurement of quantum back action in the audio band at room temperature. *Nature* **568**, 364–367 (2019).
19. Cripe, J. et al. Quantum back action cancellation in the audio band. Preprint at http://arXiv.org/abs/1812.10028 (2018).
20. Cole, G. D., Gröblacher, S., Gugler, K., Gigan, S. & Aspelmeyer, M. Monocrystalline $Al_xGa_{1-x}As$ heterostructures for high-reflectivity high-*Q* micromechanical resonators in the megahertz regime. *Appl. Phys. Lett.* **92**, 261108 (2008).
21. Cole, G. D. et al. High-performance near- and mid-infrared crystalline coatings. *Optica* **3**, 647–656 (2016).
22. Singh, R., Cole, G. D., Cripe, J. & Corbitt, T. Stable optical trap from a single optical field utilizing birefringence. *Phys. Rev. Lett.* **117**, 213604 (2016).
23. Aspelmeyer, M., Kippenberg, T. J. & Marquardt, F. Cavity optomechanics. *Rev. Mod. Phys.* **86**, 1391–1452 (2014).
24. Sheard, B. S., Gray, M. B., Mow-Lowry, C. M., McClelland, D. E. & Whitcomb, S. E. Observation and characterization of an optical spring. *Phys. Rev. A* **69**, 051801 (2004).
25. Corbitt, T. et al. An all-optical trap for a gram-scale mirror. *Phys. Rev. Lett.* **98**, 150802 (2007).
26. Cripe, J. et al. Radiation-pressure-mediated control of an optomechanical cavity. *Phys. Rev. A* **97**, 013827 (2018).
27. Wade, A. R. et al. Optomechanical design and construction of a vacuum-compatible optical parametric oscillator for generation of squeezed light. *Rev. Sci. Instrum.* **87**, 063104 (2016).
28. Drever, R. W. P. et al. Laser phase and frequency stabilization using an optical resonator. *Appl. Phys. B* **31**, 97–105 (1983).
29. Vahlbruch, H. et al. Coherent control of vacuum squeezing in the gravitational-wave detection band. *Phys. Rev. Lett.* **97**, 011101 (2006).
30. Chua, S. S. Y. et al. Backscatter tolerant squeezed light source for advanced gravitational-wave detectors. *Opt. Lett.* **36**, 4680–4682 (2011).
31. Braginsky, V. B., Vorontsov, Y. I. & Thorne, K. S. Quantum nondemolition measurements. *Science* **209**, 547–557 (1980).

32. Oelker, E. et al. Audio-band frequency-dependent squeezing for gravitational-wave detectors. *Phys. Rev. Lett.* **116**, 041102 (2016).
33. Gräf, C. et al. Design of a speed meter interferometer proof-of-principle experiment. *Class. Quantum Grav.* **31**, 215009 (2014).
34. Giovannetti, V., Lloyd, S. & Maccone, L. Quantum-enhanced measurements: beating the standard quantum limit. *Science* **306**, 1330–1336 (2004).
35. Braginsky, V. B. Classical and quantum restrictions on the detection of weak disturbances of a macroscopic oscillator. *Sov. Phys. JETP* **26**, 831 (1968).
36. Buonanno, A. & Chen, Y. Quantum noise in second generation, signal-recycled laser interferometric gravitational-wave detectors. *Phys. Rev. D* **64**, 042006 (2001).

Acknowledgements

This research was supported by the Australian Research Council under the Australian Research Council (ARC) Centre of Excellence for Gravitational Wave Discovery grant no. CE170100004 and ARC Discovery Project DP160100760. J.C. and T.C. are supported by the National Science Foundation (NSF; grants nos. PHY-1150531 and PHY-1806634). The microresonator manufacturing was carried out at the University of California, Santa Barbara (UCSB) Nanofabrication Facility. M.J.Y. thanks D. Shaddock for initial discussions.

Author contributions

M.J.Y., J.C. and T.C. performed the investigation and formal analysis. D.E.M. and T.C. performed the conceptualization. M.J.Y. wrote the original draft manuscript. J.C., T.G.M., R.L.W., D.E.M. and T.C. reviewed and edited the manuscript. G.L.M., T.G.M., P.H., D.F. and G.D.C. provided resources. T.G.M., R.L.W., B.J.J.S., D.E.M. and T.C. provided supervision.

Competing interests

The authors declare no competing interests.

Additional information

Supplementary information is available for this paper at https://doi.org/10.1038/s41566-019-0527-y.

Correspondence and requests for materials should be addressed to M.J.Y.

Reprints and permissions information is available at www.nature.com/reprints.

Publisher's note Springer Nature remains neutral with regard to jurisdictional claims in published maps and institutional affiliations.